Lattice QED in an external magnetic field: Evidence for dynamical chiral symmetry breaking

J. B. Kogut

Department of Energy, Division of High Energy Physics, Washington, DC 20585, USA and Department of Physics—TQHN, University of Maryland, 82 Regents Drive, College Park, Maryland 20742, USA

D. K. Sinclair

HEP Division, Argonne National Laboratory, 9700 South Cass Avenue, Lemont, Illinois 60439, USA

(Received 16 November 2023; accepted 11 January 2024; published 16 February 2024)

We simulate quantum electrodynamics (QED) in a strong constant homogeneous external magnetic field on a Euclidean space-time lattice using the rational hybrid Monte Carlo method, developed for simulating lattice quantum chromodynamics (QCD). Our primary goal is to measure the chiral condensate in the limit when the input electron mass m is zero. We observe a nonzero value, indicating that the external magnetic field catalyzes chiral symmetry breaking as predicted by approximate truncated Schwinger-Dyson methods. Such behavior is associated with dominance by the lowest Landau level which causes the effective dimensional reduction from $3+1$ dimensions to $1+1$ dimensions for charged particles (electrons and positrons) where the attractive forces of QED can produce chiral symmetry breaking with a dynamical electron mass and associated chiral condensate. Since our lattice simulations use bare (lattice) parameters, while the Schwinger-Dyson analyses work with renormalized quantities, direct numerical comparison will require renormalization of our lattice results.

DOI: 10.1103/PhysRevD.109.034511

I. INTRODUCTION

Theoretical studies of free electrons in external electromagnetic fields were some of the earliest applications of relativistic quantum mechanics, [1–3], and exhibited some of the features of quantum electrodynamics, such as the Sauter-Schwinger effect [1,3] (the instability of the vacuum in a strong electric field, with the production of electron-positron pairs). [For a review of those field configurations where an exact closed form solution as simple integral or series is known, see, for example, the review article by Gerald Dunne [4]].

QED (quantum electrodynamics) in strong external electromagnetic fields is of relevance to high and medium energy physics, laser and accelerator physics, astrophysics and cosmology, and condensed matter physics. See, for example, V. Yakimenko *et al.* [5], for a discussion with examples of the physics associated with QED in strong electromagnetic fields.

Current and future experiments at SLAC, LBNL, and ELI, which collide the light from petawatt lasers with electron/positron beams or plasmas, produce environments with electromagnetic fields strong enough to produce quantum and QED effects [6–8]. This requires electromagnetic fields which approach or exceed the critical values $E_{\rm cr} = m^2/e$ or $B_{\rm cr} = m^2/e$ where m and e are the electron mass and charge respectively. Another source of such strong fields is in the charged particle beams at future accelerators and their interactions, where fields could even be strong enough that the electron loop expansion (the last remnant of perturbation theory) breaks down [5]. Certain compact astronomical objects, in particular those which are sources of x- and gamma-ray emissions and are identified as neutron stars are believed to have very strong surface magnetic fields (magnetars). See for example [9]. Some have postulated the presence of very strong magnetic fields in the early universe as the source of the magnetic fields observed in the universe today.

We simulate lattice QED in external electromagnetic fields using the methods developed for simulating lattice QCD. Although some of the more interesting physics from an experimental point of view such as the Sauter-Schwinger effect—the production of electron-positron pairs from the unstable vacuum—are produced by strong external electric fields, this electric field makes the action

complex, the imaginary part describing vacuum decay. Hence standard lattice simulations cannot be applied. We therefore start with simulations of QED in external magnetic fields where the action is real and bounded below. We simulate using a non-compact gauge action and staggered fermions, using the RHMC algorithm to allow tuning to a single electron "flavor". For details see Sec. II.

We start with considering the case of "free" electrons in a constant (in space and time) magnetic field with magnitude B, comparing our lattice results with the known exact solutions [3,4] to determine the range of B or more precisely eB (e is the electron charge) over which there is good agreement.

Next we perform simulations of full lattice QED at a near-physical electron charge $\alpha = e^2/4\pi = 1/137$, on a 36^4 lattice with safe ($36m \gg 1$, $m \ll 1$) electron masses $m = 0.1$, $m = 0.2$, comparing observables with those for free ($\alpha = 0$) electrons in a magnetic field. We then perform simulations at $B = 0$ for a range of α on 36^4 lattices with $m = 0.1$, checking that the gauge action per site's α dependence is consistent with perturbation theory.

One of the theoretically most interesting predictions for QED in an external magnetic field is that the presence of this external field breaks chiral symmetry at $m = 0$. This manifests itself by giving a small dynamical mass to the electron which in turn gives rise to a non-zero chiral condensate. These predictions were obtained using truncated Schwinger-Dyson analyses, where the effects of the truncations required to obtain results, are difficult to estimate. The dynamical mass production was predicted in [10–20]. Estimates of the chiral condensates are given in [21,22] For a good review with a more complete set of references see Ref. [23]. For a more recent review, see, for example [24]. It is therefore important to check these predictions using methods whose errors are easier to estimate and which allow systematic improvements. Lattice QED simulations are of this nature. However, the best estimates of Gusynin, Miransky and Shovkovy [12] predict a dynamical electron mass at our chosen $eB = 0.4848\ldots$ and a near-physical $\alpha = 1/137$, $m_{\rm dyn} \sim 3 \times 10^{-35}$, far below anything we could measure on the lattice. Therefore we choose a stronger electron charge $\alpha = 1/5$, where the predicted $m_{\rm dyn} \approx 3 \times 10^{-4}$. Here our simulations show evidence of chiral-symmetry breaking at a level 1 to 2 orders of magnitude greater than the "best" Schwinger-Dyson results, however, our lattice QED results are for bare quantities, whereas those using Schwinger-Dyson analyses are for renormalized quantities.

Preliminary results were presented at Lattice 2021, Lattice 2022 and Lattice 2023 [25–27].

Section II defines Lattice QED in an external magnetic field. Section III compares the effects of an external magnetic field on electrons on the lattice with those in the continuum. Section IV presents simulations of Lattice QED at $\alpha = 1/137$ in an external magnetic field. Section V describes simulations of Lattice QED at $\alpha = 1/5$ in an external magnetic field. Section VI presents discussions and conclusions.

II. LATTICE QED IN AN EXTERNAL MAGNETIC FIELD

In this section we describe the lattice transcription of QED in an external magnetic field used for our simulations. (Note that here and elsewhere in this paper we work in lattice units, where the lattice spacing a is chosen to be 1. This can always be obtained from a more general choice of a by multiplying parameters and operators which have nontrivial dimensions by sufficient powers of a to make them dimensionless.) We use the noncompact gauge action

$$S(A) = \frac{\beta}{2} \sum_{n,\mu<\nu} \left[A_\nu(n+\hat{\mu}) - A_\nu(n) - A_\mu(n+\hat{\nu}) + A_\mu(n)\right]^2 \tag{1}$$

where n is summed over the lattice sites and μ and ν run from 1 to 4 subject to the restriction. $\beta = 1/e^2$. This preserves the continuum gauge group as that of 4-dimensional translations of the gauge field A_μ. The action is still quadratic in the gauge fields and hence describes a noninteracting free field. Compacting the translations to $U(1)$ introduces an extra parameter, the radius of compactification and produces an interacting theory. What is more, the strong interacting field theory becomes confining, while the weak interacting remains nonconfining. Hence the compactification produces a spurious phase transition from strong to weak coupling, a complication which we consider undesirable. As for the fermion action, gauge transformations, even in the continuum, multiply the fermion field by a phase factor, which is a compact $U(1)$ transformation, so the compact form is natural, and is the only form which is gauge invariant. The functional integral to calculate the expectation value for an observable $\mathcal{O}(A)$ is then

$$\langle \mathcal{O} \rangle = \frac{1}{Z} \int_{-\infty}^{\infty} \Pi_{n,\mu} dA_\mu(n) e^{-S(A)} \left[\det \mathcal{M}(A + A_{\rm ext})\right]^{1/8} \mathcal{O}(A) \tag{2}$$

where $\mathcal{M} = M^\dagger M$ and M is the staggered fermion action in the presence of the dynamic photon field A and external photon field $A_{\rm ext}$ describing the magnetic [16] field B (or rather eB). M is defined by

$$M(A + A_{\rm ext}) = \sum_\mu D_\mu(A + A_{\rm ext}) + m \tag{3}$$

where the operator D_μ is defined by

$$\left[D_\mu(A+A_{\rm ext})\psi\right](n) = \frac{1}{2}\eta_\mu(n)\left\{e^{i(A_\mu(n)+A_{ext,\mu}(n))}\psi(n+\hat{\mu}) - e^{-i(A_\mu(n-\hat{\mu})+A_{ext,\mu}(n-\hat{\mu}))}\psi(n-\hat{\mu})\right\} \tag{4}$$

and η_μ are the staggered phases. Note that this treatment of the gauge-field–fermion interactions is compact and so has period 2π in the gauge fields.

We implement the RHMC simulation method of Clark and Kennedy [28,29], using a rational approximation to $\mathcal{M}^{-1/8}$ and rational approximations to $\mathcal{M}^{\pm 1/16}$. (Note that, in the notation of Clark [29] Sec. III, α [not to be confused with the fine structure constant] is 1/8.) To account for the range of normal modes of the noncompact gauge action, we vary the trajectory lengths τ over the range,

$$\frac{\pi}{2\sqrt{\beta}} \le \tau \le \frac{4\pi}{\sqrt{2\beta(4-\sum_\mu \cos(2\pi/N_\mu))}}, \tag{5}$$

of the periods of the modes of this gauge action. Here N_μ is the length of the lattice in the μ direction which is chosen to be that of maximum extent [30]. (Note that we typically only change the trajectory length after a trajectory has been accepted.)

$A_{\rm ext}$ are chosen in the symmetric gauge as

$$\begin{aligned}
A_{\rm ext,1}(i,j,k,l) &= -\frac{eB}{2}(j-1) && i \neq N_1\\
A_{\rm ext,1}(i,j,k,l) &= -\frac{eB}{2}(N_1+1)(j-1) && i = N_1\\
A_{\rm ext,2}(i,j,k,l) &= +\frac{eB}{2}(i-1) && j \neq N_2\\
A_{\rm ext,2}(i,j,k,l) &= +\frac{eB}{2}(N_2+1)(i-1) && j = N_2
\end{aligned} \tag{6}$$

while $A_{\rm ext,3}(n) = A_{\rm ext,4}(n) = 0$ [31]. In practice we subtract the average values of $A_{{\rm ext},\mu}$ from these definitions. This choice produces a magnetic field eB in the $+z$ direction on every 1, 2 plaquette except that with $i = N_1$, $j = N_2$, which has the magnetic field $eB(1-N_1N_2)$. Because of the compact nature of the interaction, requiring $eBN_1N_2 = 2\pi n$ for some integer $n = 0, 1, \ldots\ldots, N_1N_2/2$ makes the value of this plaquette indistinguishable from eB. Hence $eB = 2\pi n/(N_1N_2)$ lies in the interval $[0,\pi]$.

At the end of each accepted trajectory, we subtract the multiple of $2\pi/N_\mu$ from each A_μ which reduces the magnitude of the lattice average of said A_μ to lie in the range $(-\pi/N_\mu, \pi/N_\mu]$. Since this is a gauge transformation it does not change any physics. In addition we transform to Landau gauge. Both these operations aim to prevent the gauge fields from becoming too large.

One of the observables we calculate is the electron contribution to the effective action per site $\frac{-1}{8V}\mathrm{trace}[\ln(\mathcal{M})]$. For $\ln(\mathcal{M})$ we use a (30, 30) rational approximation to the logarithm. Here we use the Chebyshev method of Kelisky and Rivlin [32]. While this has worse errors than a Remez approach, it preserves some of the properties of the logarithm itself, and is applicable on the whole complex plane cut along the negative real axis. (This would be important if we had an electric field, in which case $\det\mathcal{M}$ would be complex).

III. "FREE" ELECTRONS IN AN EXTERNAL MAGNETIC FIELD

We restrict ourselves to considering an external magnetic field of strength B which is constant in space and time and oriented in the $+z$ direction. Classically "free" electrons in such a magnetic field traverse helical orbits. The motion parallel to the magnetic field is free, while that orthogonal to the magnetic field is circular and hence bound.

Quantum mechanics restricts the motion perpendicular to the field to a discrete set of transverse energy levels known as the Landau levels [33]. As B increases, the radii of these orbits decreases. The radius of the lowest Landau level is $1/\sqrt{eB}$. This leads to an effective dimensional reduction from $3+1$ to $1+1$ dimensions for charged particles in a large magnetic field. The energy of the nth Landau level is

$$E_n = \sqrt{p_3^2 + 2eBn + m^2} \tag{7}$$

where $n = 0, 1, 2\ldots$. The degeneracy of each $n = 0$ energy level is $\frac{eB}{2\pi}\mathcal{A}_{xy}$ and that of each $n > 0$ energy level is $\frac{eB}{\pi}\mathcal{A}_{xy}$ where $\mathcal{A}_{xy}$ is the area in the xy plane.

We now calculate the chiral condensate $\langle\bar{\psi}\psi\rangle$ on the lattice for masses $m = 0.1$ and $m = 0.2$ on a 36^4 lattice, values which we use for our initial QED simulations at $\alpha = 1/137$, over a range of allowed eB values. This is to test the range of applicability of the lattice approach against the known continuum results. The lattice chiral condensate

$$\langle\bar{\psi}\psi\rangle = \frac{1}{4V}\mathrm{trace}\left[M^{-1}(A_{\rm ext})\right] \tag{8}$$

where M is defined in Sec. II. Because $A_{\rm ext}$ is independent of z and t, we only need to calculate the trace over one xy plane. In fact, for $m = 0.1$ and $m = 0.2$, all terms in the trace are almost identical. We compare this with the known continuum result:

$$\langle\bar{\psi}\psi\rangle = \langle\bar{\psi}\psi\rangle|_{eB=0} + \frac{meB}{4\pi^2}\int_0^\infty \frac{ds}{s}e^{-sm^2} \times \left[\coth(eBs) - \frac{1}{eBs}\right]. \tag{9}$$

where $\langle\bar{\psi}\psi\rangle|_{eB=0}$ is taken from the lattice. This is necessary because $\langle\bar{\psi}\psi\rangle|_{eB=0}$ depends on the UV regulator, which is

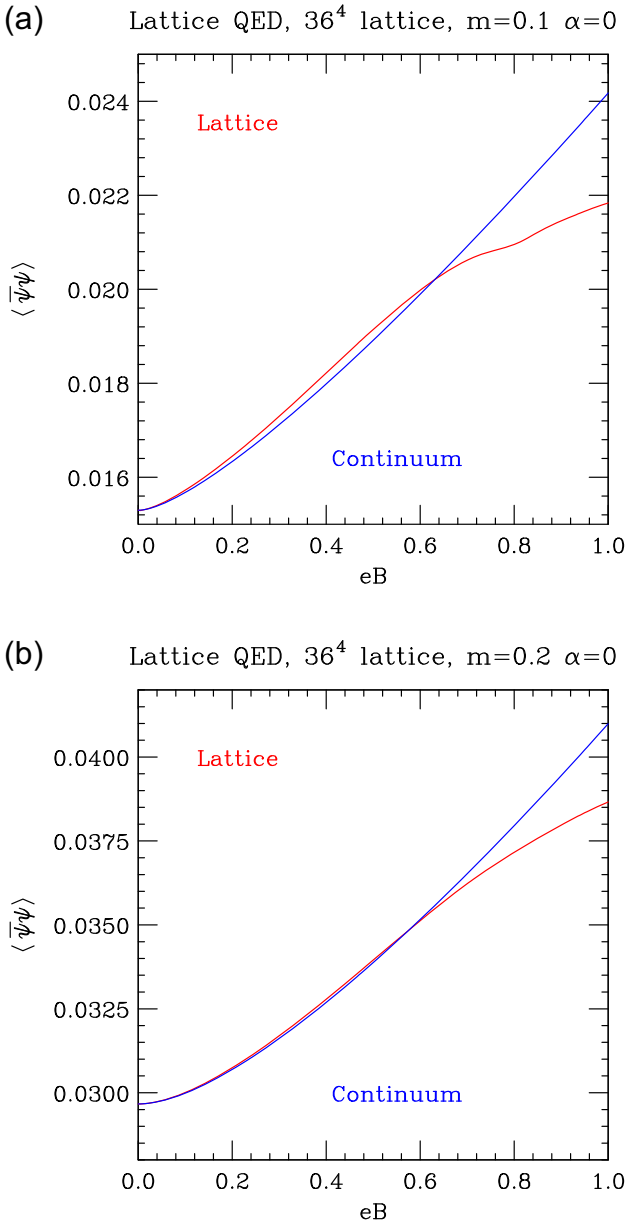

FIG. 1. Electron chiral condensates $\langle\bar{\psi}\psi\rangle$ as functions of eB, comparing the continuum and lattice results for (a) $m = 0.1$ and (b) $m = 0.2$.

different on the lattice than in the continuum. (Note that we have checked that we get the same result from Eq. (8) and from summing over the normal modes on the lattice.)

Figure 1 compares the chiral condensates for free electrons in an external magnetic field B for $m = 0.1$ and for $m = 0.2$ as functions of eB on a 36^4 lattice, and compares them with the known continuum results. We conclude that the lattice results are in acceptable agreement with the continuum results for $eB \lesssim 0.63$ for each mass.

We also calculate the fermion effective action/site on the lattice

$$\mathcal{L}_f = -\frac{1}{4V}\ln\{\det[M(A_{\rm ext})]\} = -\frac{1}{4V}\,\mathrm{trace}\{\ln[M(A_{\rm ext})]\} \tag{10}$$

which we compare with the known continuum result:

$$\mathcal{L}_f = \mathcal{L}_f|_{B=0} + \frac{(eB)^2}{24\pi^2}\int_0^\infty \frac{ds}{s}e^{-m^2 s} + \frac{eB}{8\pi^2}\int_0^\infty \frac{ds}{s^2}e^{-m^2 s}\left[\coth(eBs) - \frac{1}{eBs} - \frac{eBs}{3}\right]. \tag{11}$$

Again we replace the divergent part of this quantity in the continuum version with that of the lattice version to take into account the difference between the continuum and lattice regulators. Since the quadratically divergent part of $\mathcal{L}_f$, $\mathcal{L}_f|_{eB=0}$ is a constant (independent of eB) and the logarithmically divergent term is proportional to $(eB)^2$, while the leading contribution of the integral (the finite part) is of order $(eB)^4$, the separation of the divergent and the finite parts is straight forward in principle.

Figure 2 shows the fermion contributions to the effective action on a 36^4 lattice as functions of eB, comparing the lattice and continuum results for $m = 0.1$ and $m = 0.2$. Again, we see good agreement over a range of eB values at least as large as for the chiral condensate.

IV. LATTICE QED SIMULATIONS AT $\alpha = 1/137$

We simulate lattice QED on a 36^4 lattice using the approach presented in section II at lattice (bare) coupling $\alpha = 1/137$ and lattice (bare) masses $m = 0.1$ and $m = 0.2$. At this α, the difference between bare and renormalized parameters is small (at most a few percent), and will therefore be ignored. Hence we consider these simulations to be performed at the physical electron charge. For $m = 0.1$ we simulate over a range of allowed eB values in the interval $0 \le eB \le 2\pi \times 160/36^2 = 0.7757\ldots$, while for $m = 0.2$ we use a selection of allowed eB values in the range $0 \le eB \le 2\pi \times 200/36^2 = 0.9696\ldots$. At each eB we run for 12500 trajectories of lengths randomly chosen from the periods of the modes of the gauge action. We store a gauge configuration every 100 trajectories for future analyses. Note that, since QED probably does not have a UV completion, the action we choose should be considered to define an effective field theory. Its form is chosen to generate results consistent with QED perturbation theory with a lattice regulator.

In Fig. 3 the chiral condensates as functions of eB for $\alpha = 1/137$ are compared to those for free electrons in a magnetic field ($\alpha = 0$). In both cases the condensate for $\alpha = 1/137$ lies above that for free electrons. This was to be expected, since the attractive force between electrons and positrons in QED is predicted to enhance the chiral

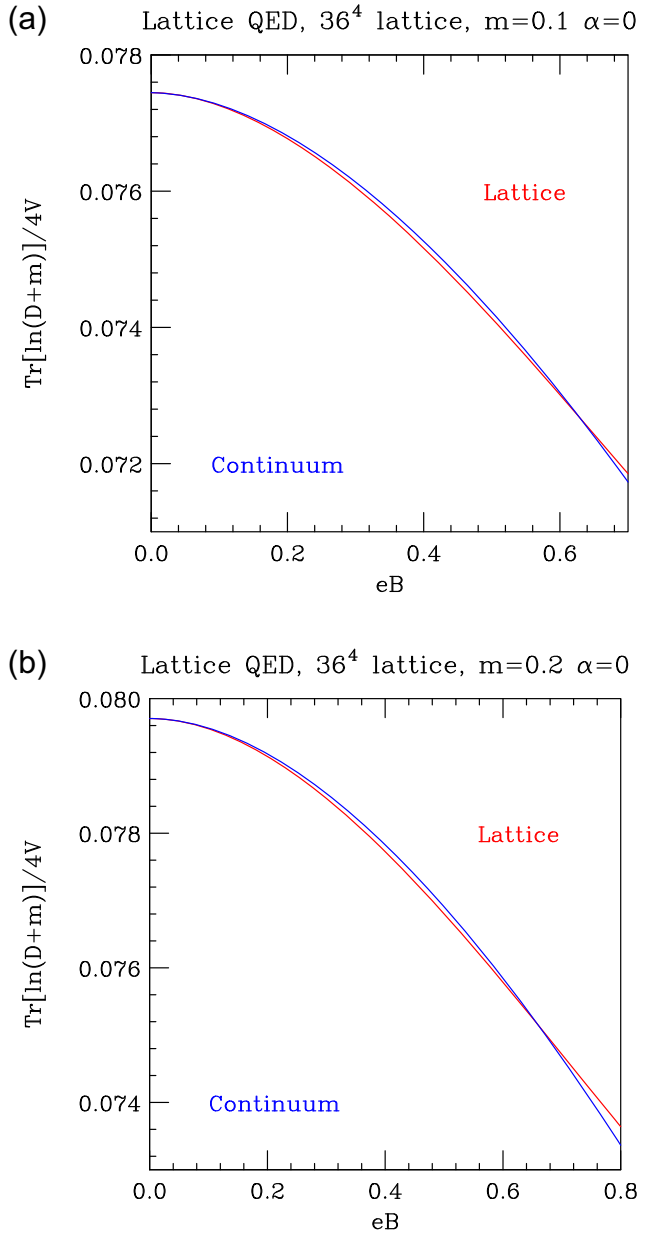

FIG. 2. Electron effective actions/site $-\mathcal{L}_f$ as functions of eB, comparing the continuum and lattice results for (a) $m = 0.1$ and (b) $m = 0.2$.

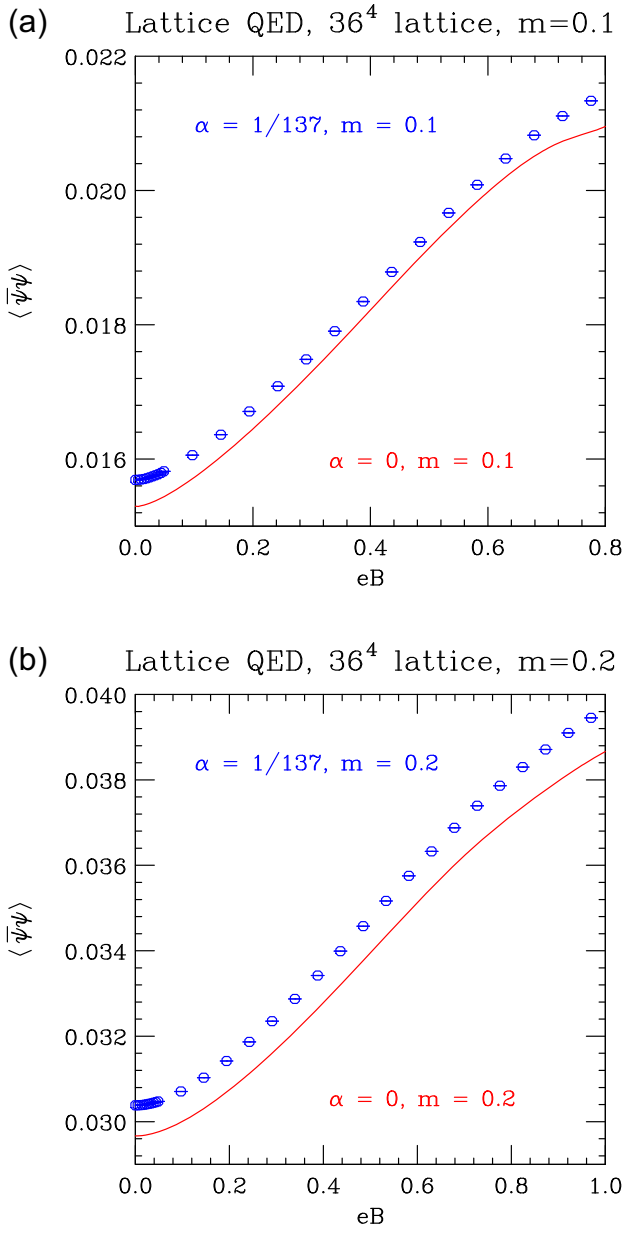

FIG. 3. Electron chiral condensates $\langle\bar{\psi}\psi\rangle$ as functions of eB, comparing the $\alpha = 1/137$ lattice results with the free-field ($\alpha = 0$) lattice results for (a) $m = 0.1$ and (b) $m = 0.2$.

condensate. A truncated Schwinger-Dyson approach indicates that chiral symmetry breaking with a dynamical electron mass proportional to $\sqrt{eB}$ and a nonzero chiral condensate proportional to $(eB)^{3/2}$ survives in the $m \to 0$ limit, however small α might be. However, at $\alpha = 1/137$, as stated in the introduction, the dynamical electron contribution to the electron mass over the range of eBs accessible to these simulations is negligible so that these measurements could be checked by lattice perturbation theory.

Figure 4 compares the effective fermion actions/site

$$\mathcal{L}_f = -\frac{1}{4V}\ln\{\det[M(A+A_{\rm ext})]\} = -\frac{1}{4V}\mathrm{trace}\{\ln[M(A+A_{\rm ext})]\} \tag{12}$$

for QED with $\alpha = 1/137$, to its free-electron value as functions of eB for $m = 0.1$ and $m = 0.2$. The effective actions for QED are well above those without QED.

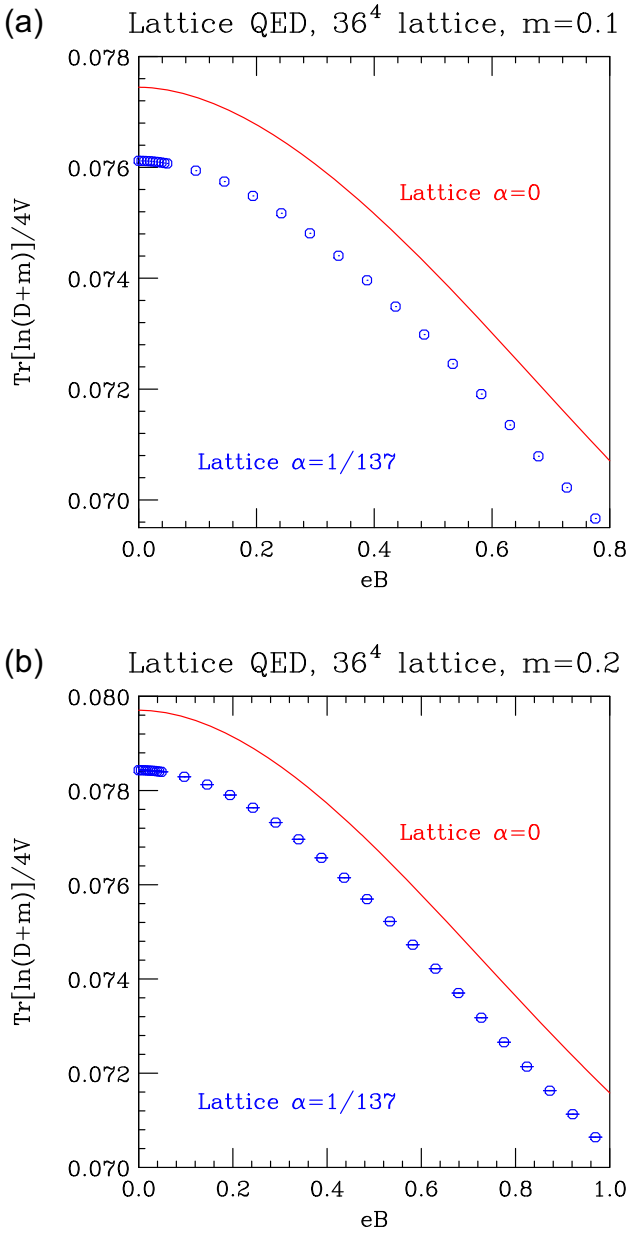

FIG. 4. Electron effective actions/site $-\mathcal{L}_f$ as functions of eB, comparing the $\alpha = 1/137$ lattice results with the free-field ($\alpha = 0$) lattice results for (a) $m = 0.1$ and (b) $m = 0.2$.

V. LATTICE QED SIMULATIONS AT $\alpha = 1/5$, $eB = 2\pi \times 100/36^2$

We are interested in finding evidence of chiral symmetry breaking for QED in (strong) external magnetic fields, which survives in the $m \to 0$ limit. Since Schwinger-Dyson analyses predict that this manifests itself as a dynamical electron mass, which at $\alpha = 1/137$ and our chosen magnetic field $eB = 0.4848\ldots$ is $m_{\rm dyn} \approx 3 \times 10^{-35}$, in the $m = 0$ limit, far below anything we could measure on the lattice, we simulate at a far stronger bare coupling, $\alpha = 1/5$. For a renormalized $\alpha = 1/5$, the predicted $m_{\rm dyn} \approx 3 \times 10^{-4}$ [12] Eq. (51). (Note that [14] Eq. (4.22) gives essentially the same result at renormalized $\alpha = 1/5$). Since equation (51) actually gives the dimensionless ratio $m_{\rm dyn}/\sqrt{2eB}$, we have inserted the value of eB in lattice units to yield $m_{\rm dyn}$ in lattice units. This leads to $\langle\bar{\psi}\psi\rangle \approx 1.2 \times 10^{-4}$, [22] equation (B4) where we have again inserted the lattice value of eB to yield a result in lattice units, which should be measurable. Of course, since our $\alpha = 1/5$ is the bare (lattice) α, there is no guarantee that it will give a measurable result, we only know this *a posteriori*. Note that, running the fine structure constant from $1/137$ at m^2 to $1/5$ indicates that the cutoff for $\alpha = 1/5$ is so large as to be beyond any physical interest. (In fact, the momentum cutoff $\Lambda_{1/5}$ with lowest order running obeys $\log(\Lambda_{1/5}/m)/\log(\Lambda_\infty/m) = (137-5)/137$, where Λ_∞ is the momentum cutoff at the Landau pole.) eB which is an order of magnitude smaller than the cutoff squared is also so large as to be only of purely theoretical interest.

First, we need to determine that $\alpha = 1/5$ is still in the range of α values where perturbation theory holds. We do this by performing simulations over a range of α values from $\alpha = 0$ to $\alpha = 1/5$. These simulations were performed at $eB = 0$ and $m = 0.1$. Our chosen observable for performing this test is the gauge Lagrangian $\mathcal{L}_\gamma$, the gauge action/lattice site. For $\alpha = 0$, $\mathcal{L}_\gamma = 1.5$ by the equipartition theorem. This value changes (decreases) only slowly with increasing α as shown in Fig. 5.

The fact that $\mathcal{L}_\gamma$ is well approximated by a low order polynomial in α with coefficients of decreasing magnitude over the range $0 \le \alpha \le 0.2$ is consistent with the claim that $\alpha = 0.2$ lies in the perturbative domain for $eB = 0$.

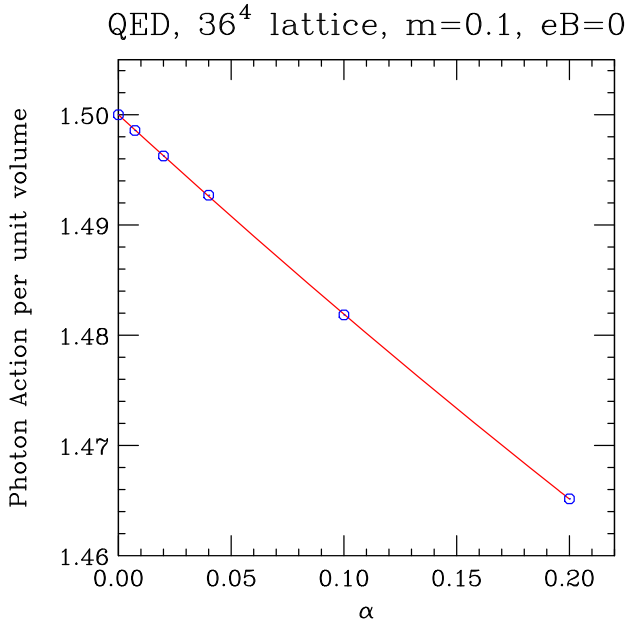

FIG. 5. Photon Lagrangian density as a function of α for $eB = 0$. The curve is the fit $\mathcal{L}_\gamma(\alpha) = 1.5 - 0.187499\alpha + 0.0661374\alpha^2$.

We have also performed simulations at $\alpha = 1$, $m = 0.1$ for which $\mathcal{L}_\gamma(1) = 1.49047(3)$, that does not appear to be consistent with perturbation theory, although one would need more simulations in the range $0.2 \leq \alpha \leq 1.0$ to check this.

Having chosen $\alpha = 1/5 = 0.2$ for our lattice QED simulations at strong coupling, we first perform simulations at $eB = 0$. Since we do not expect any chiral symmetry breaking in the $m \to 0$ limit, we expect that perturbation theory should be valid, and this means that the chiral condensate at nonzero mass will have the form $m\Lambda^2$ times some function of $\log(\Lambda^2/m^2)$, where Λ is the momentum cutoff. On the lattice, since we use units where the lattice spacing is 1, $\Lambda = \pm\pi$ in each of the 4 directions x, y, z, t. The proportionality to Λ^2 means that the trace of the propagator, which defines the chiral condensate, is dominated by large momenta and hence short distances, and should not be sensitive to the size of the lattice. The size of the lattice is probed by small momenta which probe long distances. Therefore we should be able to calculate the condensate on relatively small lattices, even in the limit as $m \to 0$. We simulate over a range of electron masses $0.001 \leq m \leq 0.2$ on a 36^4 lattice, noting that for the lowest mass $m = 0.001$, $mN_\mu = 0.036 \ll 1$, far outside the range of "safe" values for which would require $mN_\mu \gg 1$.

Figure 6 shows the chiral condensate $\langle\bar{\psi}\psi\rangle$ as a function of m on a 36^4 lattice for $\alpha = 1/5$. This graph also shows the value of the chiral condensate at the lowest mass, $m = 0.001$, from a simulation on a larger (48^4) lattice, which shows no sign of any appreciable dependence on lattice size. In fact, $\langle\bar{\psi}\psi\rangle(m = 0.001) = 4.3259(7) \times 10^{-4}$ on a 36^4 lattice compared with $\langle\bar{\psi}\psi\rangle(m = 0.001) = 4.3294(7) \times 10^{-4}$ on a 48^4 lattice. A simple linear extrapolation from the lowest 2 masses ($m = 0.001$,$m = 0.005$), which because of the curvature of this graph, should yield an upper bound to the value at $m = 0$, predicts $\langle\bar{\psi}\psi\rangle_{m=0} = 5(1) \times 10^{-7}$, a value which curvature can easily lower to zero. Hence the chiral condensate at $m = 0$ for $\alpha = 1/5$ and $eB = 0$ is consistent with zero.

To search for evidence of chiral symmetry breaking at $m = 0$ catalyzed by a strong magnetic field we perform simulations at $\alpha = 1/5$ and $eB = 2\pi \times 100/36^2 = 2\pi \times 25/18^2 = 0.4848\ldots$, relatively large, while being significantly below $eB = 0.63$ above which measurements of chiral condensates on the lattice for free fermions in an external magnetic field show appreciable departures from known continuum values. Here we need to make measurements at m values small enough that our 36^4 lattice is too small to yield infinite lattice values for the chiral condensate. However, the assumption that for large eB only the lowest Landau levels (LLL) make significant contributions to physics means that as long as the lattice projection in the xy plane is considerably larger than that of the LLL, whose radii are $\approx 1/\sqrt{eB}$, then the chiral condensates should not depend on $N_x = N_y$, no matter how small m becomes. For this reason we fix $N_x = N_y = 36$ or $N_x = N_y = 18$ for our simulations. Here we have checked for a limited number of $N_z = N_t$ (36 and 64) that there is consistency between $N_x = N_y = 36$ and $N_x = N_y = 18$ and hence that the remaining massless particle (the photon) does not affect this conclusion. For large eB the charged particles are thus restricted to $1 + 1$ dimensions (z and t). Since these $1 + 1$ dimensional electrons and positrons are free to move in the z and t directions one can expect that, at small mass, the chiral condensates will depend on the lattice extents in the those directions until $N_z = N_t$ exceeds the new scale associated with chiral symmetry breaking. Were it not

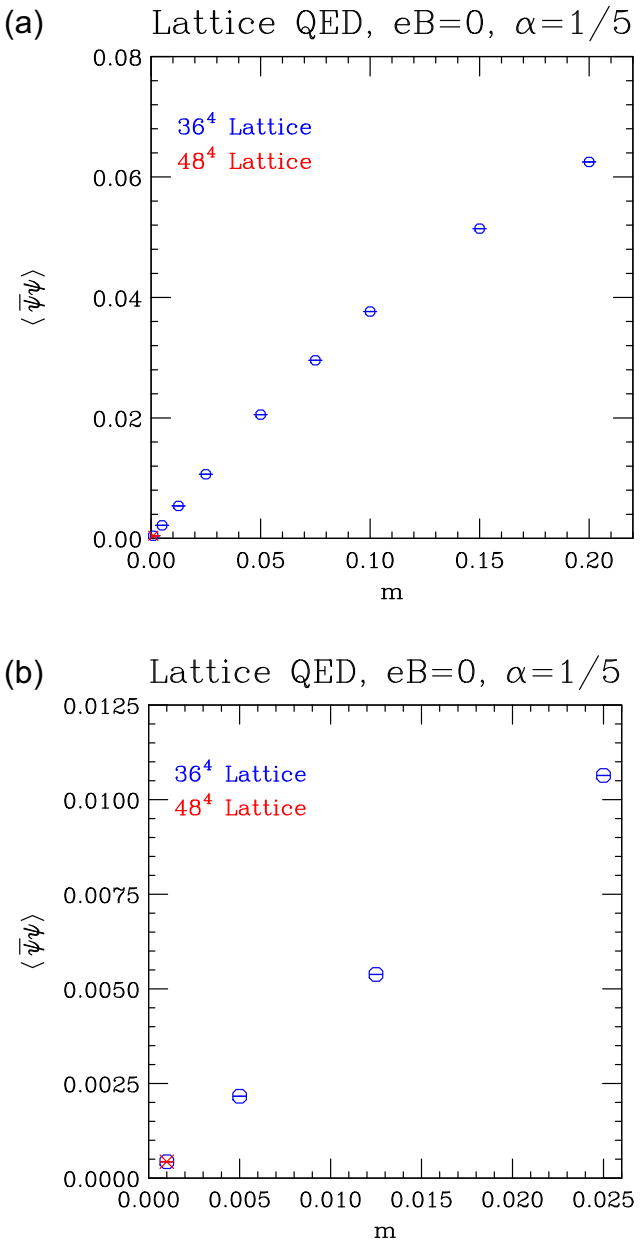

FIG. 6. Electron chiral condensates $\langle\bar{\psi}\psi\rangle$ as functions of m for $\alpha = 0$, $eB = 0$: (a) full mass range, (b) low mass region.

for QED, chiral symmetry would not be broken in the limit $m \to 0$ unlike what occurs in $2+1$ dimensions. The relatively weak QED interactions in the z and t directions can cause chiral symmetry breaking, giving dynamical masses to the electrons and nonzero chiral condensates at $m = 0$. In the limit as $m \to 0$, the dynamical masses can only be proportional to $\sqrt{eB}$ and the condensates to $(eB)^{3/2}$. eB gives the new intermediate or infrared scale for chiral symmetry breaking as our simulations indicate.

We perform simulations at a selection of m values in the range $0.001 \le m \le 0.2$, starting with a 36^4 lattice at each mass. At the lower masses we then increase the lattice size to $36^2 \times 64^2$ and also consider $18^2 \times 64^2$ at $m = 0.001$ for comparison. Because at $m = 0.025$, the increase in the chiral condensate in going from a 36^4 lattice to a $36^2 \times 64^2$ lattice is very small, we conclude that a 36^4 lattice would have been adequate, and that it is unnecessary to increase the lattice sizes for any $m > 0.025$. For $m = 0.0125$ there is a small but significant increase in the chiral condensate in going from a 36^4 lattice to a $36^2 \times 64^2$ lattice, from which we conclude that a 36^4 lattice is too small, but a $36^2 \times 64^2$ lattice is probably adequate. For $m = 0.005$ we conclude that a $36^2 \times 96^2$ lattice is adequate while for $m = 0.001$ we needed the $18^2 \times 128^2$ lattice.

Figure 7 shows the chiral condensates as functions of mass at $\alpha = 1/5$ for $eB = 2\pi \times 100/36^2 = 2\pi \times 25/18^2 = 0.4848\ldots$. This strongly suggests that the condensates approach a finite, non-zero limit as $m \to 0$. From the obvious curvature of this graph (through the uppermost point at each m), a straight line through the points for the 2 lightest masses will pass through $m = 0$ at a point marking an upper bound to the $m = 0$ condensate. This value is $3.977\ldots \times 10^{-3}$. To estimate a lower bound, we need to fit a smooth curve to the condensates for the smallest masses for which we have simulations. This requires choosing a functional form which displays increasing curvature as $m \to 0$, and fitting it to the condensates for the lowest masses. The first form we choose is: $f(m) = a + bm + cm\log(m) + dm^2$. Fitting this to the condensates at $m = 0.001$, $m = 0.005$, $m = 0.0125$ and $m = 0.025$ gives values for a, b, c, d. The zero mass intercept is $a = 3.45\ldots \times 10^{-3}$. Adding more points to the fit increases the $m = 0$ intercept. The curvature shows the expected behavior. Setting $d = 0$ and fitting only the points $m = 0.001$, $m = 0.005$, and $m = 0.0125$ raises the intercept slightly to $a = 3.5097\ldots \times 10^{-3}$, and suggests setting $c = b$ and only using $m = 0.001$, $m = 0.005$ for the fit. Thus we have reduced $f(m)$ to $f(m) = a + bm(1 + \log(m))$. This lowers the intercept slightly to $a = 3.50565 \times 10^{-3}$. Including the point at $m = 0.0125$ to the fit changes the parameters a and b only slightly and gives an excellent fit ($\chi^2/DOF \approx 0.7$). We now consider an alternative fit to $f(m) = a + bm^c$. Fitting this to the condensates at $m = 0.001$, $m = 0.005$, $m = 0.0125$ yields an intercept $a \approx 3.16 \times 10^{-3}$. Adding the point at $m = 0.025$ to the fit gives an excellent fit ($\chi^2/DOF \approx 0.5$), lowers the intercept to $a \approx 3.14 \times 10^{-3}$ and makes slight changes to b and c). In conclusion, a conservative estimate of the condensate at $m = 0$ is that it lies in the range:

$$3 \times 10^{-3} \le \langle \bar{\psi}\psi \rangle_{m=0} < 4 \times 10^{-3}$$

This compares with the "best" Schwinger-Dyson estimates for the chiral condensate at $\alpha = 1/5$, $eB = 0.4848\ldots$, $N_f = 1$, $m = 0$, which predicts that $\langle \bar{\psi}\psi \rangle_{m=0} \approx 1.2 \times 10^{-4}$. Of course, a direct comparison is not possible

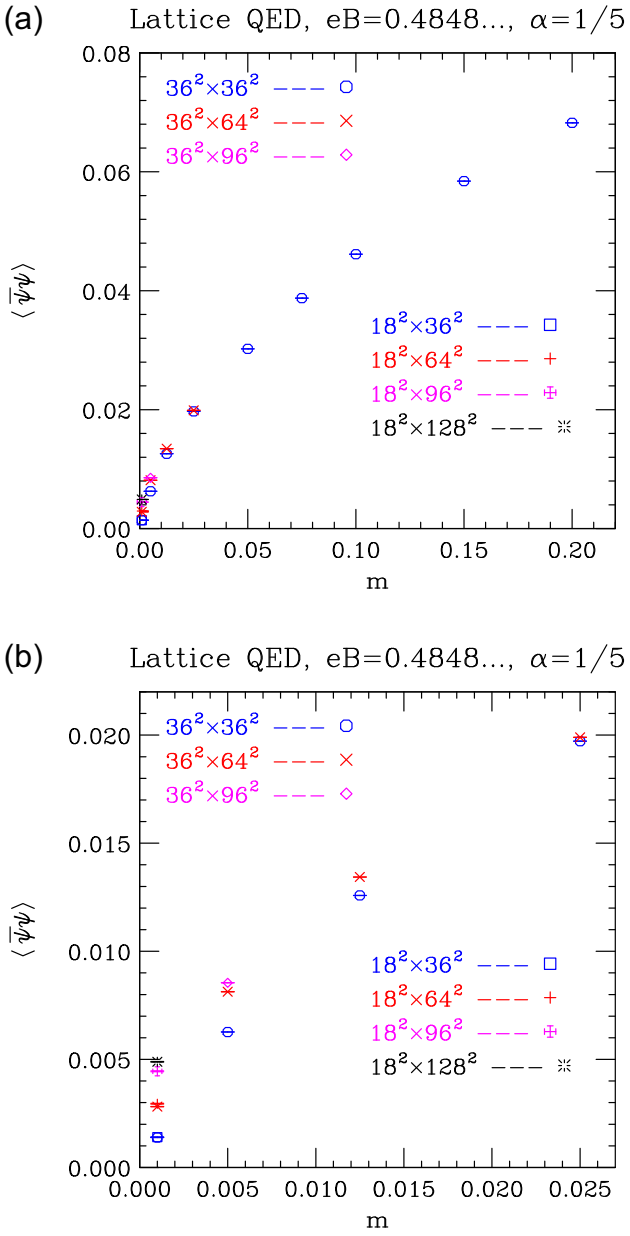

FIG. 7. Electron chiral condensates $\langle \bar{\psi}\psi \rangle$ as functions of m for $\alpha = 0$, $eB = 2\pi \times 100/36^2$: (a) full mass range, (b) low mass region.

because the parameters in the lattice are bare (lattice) parameters, while those in the Schwinger-Dyson estimates are renormalized quantities. We discuss this further in the Discussion and Conclusions section.

VI. DISCUSSION AND CONCLUSIONS

We simulate lattice QED in a strong external magnetic field using the RHMC method developed for simulating lattice QCD. Much of our effort is aimed at seeking evidence for chiral symmetry breaking in the limit that the lattice (bare) mass approaches zero, catalyzed by the external magnetic field, as predicted by less reliable truncated Schwinger-Dyson analyses. Such chiral symmetry breaking is facilitated in part by the electrons and positrons preferentially occupying the lowest Landau level (LLL) with its radius $1/\sqrt{eB}$ due to the external magnetic field causing an effective dimensional reduction from $3+1$ to $1+1$ for charged particles. The attractive force due to QED then produces chiral symmetry breaking. The broken chiral symmetry manifests itself by producing a dynamical mass for the electron and a non-zero chiral condensate.

We simulate Lattice QED in a constant (in space and time) external magnetic field $\boldsymbol{B}$, ($e\boldsymbol{B} = \boldsymbol{\nabla} \times \boldsymbol{A}_{\mathbf{ext}}$), with staggered electrons, using the RHMC method. We choose the bare $\alpha = e^2/4\pi = 1/5$, $eB = 2\pi \times 100/36^2 = 0.4848\ldots$ and a range of electron masses and lattice sizes sufficient to extrapolate the chiral condensate $\langle\bar{\psi}\psi\rangle$ to $m = 0$. We estimate $\langle\bar{\psi}\psi\rangle = 3\text{–}4 \times 10^{-3}$ at $m = 0$, definitely non zero, indicating that chiral symmetry is broken. Note that the parameters and fields in the action are bare lattice quantities. This compares with the renormalized condensate of $\approx 1.2 \times 10^{-4}$ from the best Schwinger-Dyson estimates. The lowest non-trivial contributions to the renormalization constants evaluated at $p^2 = m_{\mathrm{dyn}}^2$ are typically $\mathcal{O}(\alpha \log(\Lambda^2/m_{\mathrm{dyn}}^2)) \approx 1\text{–}3$ where $\Lambda \approx \pi$ is the momentum cutoff on the lattice. If instead one chooses to renormalize at momentum scale μ with $\mu^2 = eB$, these contributions are reduced to $\mathcal{O}(\alpha \log(\Lambda^2/eB)) \approx 0.6$. In either case, renormalization cannot be ignored. This contrasts with our simulations with $\alpha = 1/137$, $m = 0.1, 0.2$, where the renormalization constants are evaluated at $p^2 = m^2$, so the lowest non-trivial order corrections are typically $\mathcal{O}(\alpha \log(\Lambda^2/m^2) \approx 0.05, 0.04)$ and can be ignored if one can tolerate errors of a few percent (in actual fact for our external magnetic fields the errors are somewhat smaller than this). There are two ways that one might check the consistency between the Schwinger-Dyson approach and the Lattice QED simulations. The first is to follow the methods developed for renormalizing lattice QCD. The dimensional reduction from $3+1$ to $1+1$ dimensions caused by the external magnetic field adds extra complications. The second approach is to repeat the Schwinger-Dyson analysis on the lattice action based on methods developed for lattice perturbation theory, in terms of bare parameters. Of course, it would be best to use both methods.

Experience with lattice QCD indicates that we should expect large taste breaking effects from the use of staggered fermions (and, in particular, rooted staggered fermions). See for example the review article [34], and its guide to the literature. In lattice QCD these effects are, to lowest order, $\mathcal{O}(a^2\Lambda_{\mathrm{QCD}}^2)$ where a is the lattice spacing. For lattice QED in an external magnetic field these effects should be, to lowest order $\mathcal{O}(a^2 eB)$ or, since we have chosen $a = 1$, $\mathcal{O}(eB)$. Hence we should be able to reduce taste breaking by reducing the external magnetic field. We are therefore repeating our simulations with a smaller magnetic field. Another way one can see that this should decrease errors is to note that with a smaller magnetic field, the lowest Landau level covers more lattice sites so that discretization errors should be reduced. With the smaller magnetic field, we should be able to test that the chiral condensate scales as $(eB)^{3/2}$ as predicted.

It would be interesting to apply lattice simulations to QED with $N_f = 2$ flavors in an external magnetic field, where such chiral symmetry breaking would imply spontaneous dynamical breaking of flavor symmetry with associated Goldstone bosons. Note that these Goldstone bosons are uncharged and hence reside in $3+1$ dimensions and therefore spontaneous breaking of continuous chiral symmetry is allowed despite the electrons being restricted to $1+1$ dimensions.

One of the first calculations planned for stored configurations is to measure the effect that QED in an external magnetic field has on the Coulomb field of a point charge in said magnetic field. It has been predicted that the Coulomb field will be partially screened and distorted by the presence of the external magnetic field [35–38]. This effect can and will be measured on our stored configurations at $\alpha = 1/137$ where renormalization can be safely ignored, with expected errors of at most a few percent. Such an analysis will be performed using Wilson loops, possibly with smearing.

We plan to calculate electron propagators on our stored configurations with $\alpha = 1/5$, $eB = 0.4848\ldots$ on lattice sizes from $36^2 \times 64^2$ to $18^2 \times 128$ to extract the electron mass extrapolated to $m = 0$. When configurations from our current and ongoing simulations at $eB = 0.1163\ldots$ become available we will then be able to check that $m_{\mathrm{dyn}} \propto \sqrt{eB}$, and extract the electron wave function renormalization constant. We will also attempt to calculate the photon propagator, although this will be considerably more difficult, since its falloff with separation of its endpoints will be statistics limited.

The one parameter left to calculate will be the renormalized coupling constant which, unless this can be calculated perturbatively, might well require additional simulations.

Of at least as much interest is the behavior of QED in an external electric field, which exhibits the Sauter-Schwinger

effect. As pointed out earlier, this has a complex action and traditional lattice simulations which rely on importance sampling cannot be used. A good starting point is to simulate lattice QED with both external electric and magnetic fields where these fields are obtained by a boost from a pure external magnetic field, since the physics should be the same as that for this magnetic field alone. One method we might try is a complex Langevin (CLE) simulation. This has some chance of succeeding for QED in external electric fields or electric and magnetic fields, whereas it failed for QCD in a quark-number chemical potential, because for pure non-compact $U(1)$ lattice gauge theory, which is a free field theory and hence a collection of harmonic oscillators, the real trajectory is an attractive fixed-point of the CLE, while for pure compact $SU(3)$ lattice gauge theory it is a repulsive fixed point. We will first need to check if the real trajectory remains an attractive fixed point for the $U(1)$ lattice gauge theory CLE simulation when the electron fields are included making it lattice QED, but without the external electric fields. If so, we plan to try CLE when the external electric or electric and magnetic fields are added.

ACKNOWLEDGMENTS

D. K. S.'s research is supported in part by U.S. Department of Energy, Division of High Energy Physics, under Contract No. DE-AC02-06CH11357. The high performance computing was provided by the LCRC at Argonne National Laboratory on their Bebop cluster. Access to Stampede-2 at TACC, Expanse at UCSD and Bridges-2 at PSC was provided under an XSEDE/ACCESS allocation. Time on Cori and Perlmutter at NERSC was provided through an ERCAP allocation and from early user access to Perlmutter during its pre-acceptance period. D. K. S. thanks G. T. Bodwin for insightful discussions, while J. B. K. would like to thank V. Yakimenko for discussions which helped inspire this project, and I. A. Shovkovy for helpful discourse on magnetic catalysis.

[1] F. Sauter, Über das Verhalten eines Elektrons im homogenen elektrischen Feld nach der relativistischen Theorie Diracs, Z. Phys. **69**, 742 (1931).
[2] W. Heisenberg and H. Euler, Folgerungen aus der Diracschen Theorie des Positrons, Z. Phys. **98**, 714 (1936).
[3] J. S. Schwinger, On gauge invariance and vacuum polarization, Phys. Rev. **82**, 664 (1951).
[4] G. V. Dunne, The Heisenberg-Euler effective action: 75 years on, Int. J. Mod. Phys. A **27**, 1260004 (2012).
[5] V. Yakimenko, S. Meuren, F. Del Gaudio, C. Baumann, A. Fedotov, F. Fiuza, T. Grismayer, M. J. Hogan, A. Pukhov, L. O. Silva *et al.*, Prospect of studying nonperturbative QED with beam-beam collisions, Phys. Rev. Lett. **122**, 190404 (2019).
[6] L. Fedeli, A. Sainte-Marie, N. Zaïm, M. Thévenet, J. L. Vay, A. Myers, F. Quéré, and H. Vincenti, Probing strong-field QED with Doppler-boosted petawatt-class lasers, Phys. Rev. Lett. **127**, 114801 (2021).
[7] S. Meuren, D. A. Reis, R. Blandford, P. H. Bucksbaum, N. J. Fisch, F. Fiuza, E. Gerstmayr, S. Glenzer, M. J. Hogan, C. Pellegrini *et al.*, MP3 White Paper 2021—Research opportunities enabled by co-locating multi-petawatt lasers with dense ultra-relativistic electron beams, arXiv:2105.11607.
[8] T-P. Yu, F. Pegoraro, G. Sarri, and D. A. Reis, Introduction to the topical issue high field QED physics, Eur. Phys. J. D **77**, 55 (2023).
[9] A. K. Harding and D. Lai, Physics of strongly magnetized neutron stars, Rep. Prog. Phys. **69**, 2631 (2006).
[10] V. P. Gusynin, V. A. Miransky, and I. A. Shovkovy, Dimensional reduction and dynamical chiral symmetry breaking by a magnetic field in $(3+1)$-dimensions, Phys. Lett. B **349**, 477 (1995).
[11] V. P. Gusynin, V. A. Miransky, and I. A. Shovkovy, Dimensional reduction and catalysis of dynamical symmetry breaking by a magnetic field, Nucl. Phys. **B462**, 249 (1996).
[12] V. P. Gusynin, V. A. Miransky, and I. A. Shovkovy, Theory of the magnetic catalysis of chiral symmetry breaking in QED, Nucl. Phys. **B563**, 361 (1999).
[13] V. P. Gusynin, V. A. Miransky, and I. A. Shovkovy, Physical gauge in the problem of dynamical chiral symmetry breaking in QED in a magnetic field, Found. Phys. **30**, 349 (2000).
[14] C. N. Leung and S. Y. Wang, Gauge independent approach to chiral symmetry breaking in a strong magnetic field, Nucl. Phys. **B747**, 266 (2006).
[15] C. N. Leung and S. Y. Wang, Gauge independence and chiral symmetry breaking in a strong magnetic field, Ann. Phys. (Amsterdam) **322**, 701 (2007).
[16] C. N. Leung, Y. J. Ng, and A. W. Ackley, Schwinger-Dyson equation approach to chiral symmetry breaking in an external magnetic field, Phys. Rev. D **54**, 4181 (1996).
[17] J. Alexandre, K. Farakos, and G. Koutsoumbas, QED in a strong external magnetic field: Beyond the constant mass approximation, Phys. Rev. D **62**, 105017 (2000).
[18] J. Alexandre, K. Farakos, and G. Koutsoumbas, Remark on the momentum dependence of the magnetic catalysis in QED, Phys. Rev. D **64**, 067702 (2001).
[19] S. Y. Wang, Dynamical electron mass in a strong magnetic field, Phys. Rev. D **77**, 025031 (2008).
[20] K. Hattori, K. Itakura, and S. Ozaki, Anatomy of the magnetic catalysis by renormalization-group method, Phys. Lett. B **775**, 283 (2017).
[21] I. A. Shushpanov and A. V. Smilga, Quark condensate in a magnetic field, Phys. Lett. B **402**, 351 (1997).

[22] D. S. Lee, C. N. Leung, and Y. J. Ng, Chiral symmetry breaking in a uniform external magnetic field, Phys. Rev. D **55**, 6504 (1997).
[23] V. A. Miransky and I. A. Shovkovy, Quantum field theory in a magnetic field: From quantum chromodynamics to graphene and Dirac semimetals, Phys. Rep. **576**, 1 (2015).
[24] K. Hattori, K. Itakura, and S. Ozaki, Strong-field physics in QED and QCD: From fundamentals to applications, Prog. Part. Nucl. Phys. **133**, 104068 (2023).
[25] D. K. Sinclair and J. B. Kogut, Lattice QED in external electromagnetic fields, Proc. Sci. LATTICE2021 (**2022**) 202 [arXiv:2111.01990].
[26] D. Sinclair and J. B. Kogut, Chiral symmetry breaking in QED induced by an external magnetic field, Proc. Sci. LATTICE2022 (**2023**) 399 [arXiv:2210.10863].
[27] D. K. Sinclair and J. B. Kogut, Lattice QED in external EM fields (to be published).
[28] M. A. Clark and A. D. Kennedy, Accelerating dynamical fermion computations using the rational hybrid Monte Carlo (RHMC) algorithm with multiple pseudofermion fields, Phys. Rev. Lett. **98**, 051601 (2007).
[29] M. A. Clark, The rational hybrid Monte Carlo algorithm, Proc. Sci. LAT2006 (**2006**) 004 [arXiv:hep-lat/0610048].
[30] S. J. Hands, A. Kocic, J. B. Kogut, R. L. Renken, D. K. Sinclair, and K. C. Wang, Spectroscopy, equation of state and monopole percolation in lattice QED with two flavors, Nucl. Phys. **B413**, 503 (1994).
[31] J. Alexandre, K. Farakos, S. J. Hands, G. Koutsoumbas, and S. E. Morrison, QED(3) with dynamical fermions in an external magnetic field, Phys. Rev. D **64**, 034502 (2001).
[32] R. P. Kelisky and T. J. Rivlin, A rational approximation to the logarithm, Math. Comput. **22**, 128 (1968).
[33] A. I. Akhiezer and V. B. Berestetsky, *Quantum Electrodynamics* (Interscience, New York, 1965).
[34] A. Bazavov *et al.* (MILC Collaboration), Nonperturbative QCD simulations with $2+1$ flavors of improved staggered quarks, Rev. Mod. Phys. **82**, 1349 (2010).
[35] A. E. Shabad and V. V. Usov, Modified Coulomb law in a strongly magnetized vacuum, Phys. Rev. Lett. **98**, 180403 (2007).
[36] A. E. Shabad and V. V. Usov, Electric field of a point-like charge in a strong magnetic field and ground state of a hydrogen-like atom, Phys. Rev. D **77**, 025001 (2008).
[37] N. Sadooghi and A. Sodeiri Jalili, New look at the modified Coulomb potential in a strong magnetic field, Phys. Rev. D **76**, 065013 (2007).
[38] B. Machet and M. I. Vysotsky, Modification of Coulomb law and energy levels of the hydrogen atom in a superstrong magnetic field, Phys. Rev. D **83**, 025022 (2011).